Enhancing the operation of smart inverters with PMU and data concentrators

Enhancing the Operation of Smart Inverters with PMU and Data Concentrators

Ameen Gargoom[a]*, Mohammed Elmusrati[b], and Ahmed Gaouda[c]

[a]*Centre for smart power and energy research (cSPER), Deakin University, Geelong, Australia*
[b]*School of Technology and Innovations, University of Vaasa, Finland*
[c]*University of Waterloo, Waterloo, ON N2L 3G1, Canada*

Abstract

As inverter-based distributed energy resources (DERs) continue to proliferate in the distribution systems and provide a significant part of the generation, enhancing the visibility of the system for coupling transmission and distribution networks is becoming essential. The paper offers a monitoring and managing approach based on integrating information from synchrophasors and phasor data concentrators (PDCs) to enhance the deployment of the smart inverter, post their dynamic functions and overcome the decoupling between distribution/transmission operations. The proposed approach includes DER monitoring and managing entity (DER-MME) which communicates with PDC units that can manage the smart inverters functions in real-time during normal/abnormal operation based on a proposed fault detection and localization algorithm. Although the approach can be expanded to include several functions, in the paper, the focus was on the momentary cessation function (MC) and how it can be dynamically controlled by the proposed approach to improve the response of smart inverters. The merit of the proposed approach has been illustrated on several transmission and distribution faults that triggered fault-induced delayed voltage recovery (FIDVR) events which are common in distribution networks.

Keywords: Smart inverters; phasor measurement unit (pmu); distributed energy resource (DER); fault-induced delayed voltage recovery (FIDVR); momentary cessations (MC); IEEE Std. 1547-2018.

1. Introduction

There is a continuous change in the distribution system that would demand more resilient, robust, adaptive, and flexible characteristics. This change is due to the high penetration levels of distributed energy resources, energy storage systems, and emerging technology. Furthermore, customer engagement, as a prosumer, becomes an essential element for the electric utilities and energy market [1]. With the high penetration of smart inverter-based distributed energy resources (SI-DERs), more automation and system integration become essential in order to monitor, in real-time, the system main variables at the distribution substations and SI-DERs terminals [2]. Having such information will allow distribution system operators (DSO) to take prompt actions that secure a reliable and continuous operation of SI-DERs as well as coordinate with transmission system operators (TSO) during steady-state, dynamic, and transient events [3]. In addition, the continuously increasing penetration of SI-DERs makes a significant part of the reactive power resources connected to the transmission network (TN) is replaced by the deployment of SI-DERs in the distribution

network (DN) [4], [5]. While the analyses, (and simulations) of the DN and TN have been traditionally decoupled due to the insignificant impact of the dynamics in the DN on the TN, the high penetration of the DERs has largely amplified the system dynamics and, thus, the shared impacts between DN and TN. Hence the TN/DN decoupling is no longer permissible as a significant generation is located on the distribution system. This entails more active participation of DNs as their geographical distribution nature may provide more flexible and localized support to the TN during normal and abnormal operations. Furthermore, the increasing coupling between the TN and DN, in terms of the increased shared dynamic impacts, urges TSO and DSO to have further visibility to ensure a precise operation of the DER which contributes to the effective system operation, control, and protection on both TN and DN sides [6]. Therefore, the deployment of advanced technology for system integrity is an important factor to ensure smart coordination and effective contribution of the SI-DERs to provide quality voltage to customer loads [7], [8].

Against this backdrop, the IEEE std. 1547-2018 [9], established criteria and requirements for interconnection of DERs with electric power systems (EPSs) and associated interfaces. The standard categorizes the performance capabilities needed for area-EPS during normal and abnormal operations. The standard supports interoperability and provides the area-EPS operator and DER operator with communication capabilities. These updates provide a new opportunity that encourages the deployment of advanced technology at the distribution level aiming for effective intelligent area-EPS integrity and provides TN/DN combined fields of monitoring, control, and protection. According to the IEEE std., SI-DERs should be capable of operating at different modes by regulating their output active and reactive power to support the network dynamics. For instance, the current exchange of the DERs with the Area-EPS during disturbances should be minimized using the momentary cessation (MC) mode which ceases the SI-DERs to energize the grid [9]. In the amended version of the IEEE std. 1547, inverters should enter the MC mode when the terminal voltage is less than 0.5 pu for up to 1 s or if the voltage is above 1.1 pu for up to 12 s. This mode, however, was initially introduced in 2015 in response to new requirements in California Rule 21 and Hawaii Rule 14H for addressing the "smart inverters" functionality [10]. The introduction of the MC mode was mainly driven by the safety requirements from distribution level perspectives during disturbances. The MC mode retains inverters galvanically connected during transient low voltage events which allows the rapid and autonomous restoration of the power if the voltage recovers within a specified time. Therefore, while ensuring safety during faults, the MC mode is used to avoid the long disconnection time (up to 5 min [11]) if an inverter was unnecessarily tripped.

However, due to the increased coupling between the TNs and DNs, voltage/frequency variations on the local terminals seen by inverters can be due to disturbances on different parts on the network (pulk-EPS, area-EPS, or local-EPS). Thus, the lack of such details on the source of the disturbance can pose a challenge to the inverters' operation to optimally support the grid. For example, inverters could trigger the MC mode based on voltage/frequency variations without identifying the type of fault (momentary/temporary) and its location (on their own DN feeder, adjacent feeder, or on the TN) which could impact the system adversely. It has been reported in [12]-[14] that in systems with high penetration of SI-DERs, the distribution and transmission systems can be critically affected by MC operation. Cases in point are the Blue Cut Fire and the Canyon Fire 2 events due to TN faults [15]. The impact of the faults in these events, although the faults were promptly cleared, has caused large losses of the PV generations (1,200 MW were lost in the Blue Cut event and 900 MW were lost in the Canyon event). Those losses in the PV generations were found primarily due to the triggering of the MC mode of large number of inverters during and following the events [12]. More incidents have been also reported in [16] where faults on the TN have caused the loss of PV generation due to inverters' responses. Those events have raised the question for a better coordination between inverters, not only in the transmission level, but also in the distribution level [16], [17].

In addition, at the load side, when the SI-DERs at both TN/DNs enter the MC and cease power contribution, the system load becomes unbalanced as compared with TN bulk generation which leads to instable operation. Furthermore, investigations conducted by [18], [19], on the response of small-scale PV inverters to short-duration voltage sags, do highlight the impact of losing DERs and the significant increase in loads due to the loss of the after-the-meter inverters. During TN or DN voltage disturbances, the MC mode causes a significant amount of rooftop DERs to drop (ceases current) at the time of disturbance and return to normal after a specific time [19]. This loss/return results in a dynamic increase in the load during the transient event and negatively affects conventional generators [12]. These impacts can be seen as rapid frequency excursions and their associated stability issues, mainly as result of the sudden unbalance in the mechanical and electrical power of the conventional generators.

Furthermore, faults in areas with high penetration of residential air conditioners (RACs) provoke fault induced delayed voltage recovery (FIDVR) events [20]. During this event, the RACs stall within 3 cycles when the voltage momentarily goes below approximately 50% causing large reactive power demand which leads to delayed voltage recovery [21]. This voltage reduction might impact all the inverters connected at the area-EPS, local-EPS, and after the meters (rooftop DERs) and drive them to MC or trip (if the low voltage persists beyond the MC time identified by the standard) which further deteriorates the voltage profile [16]. Moreover, this voltage deterioration drives more RAC loads to stall and generate undesirable dynamic load behavior. Consequently, there is a concern that faults and transient events at the TN can cause a loss of significant part rooftop DERs and stall RAC units at a wide area of the DN. Such an event can have a detrimental impact on the loss of a significant amount of inverter-based DERs and develop a stability problem.

It has been reported in [22], [23] that faults resulted in the loss of a significant amount of solar photovoltaic (PV) generation. These events were monitored by a supervisory control and data acquisition (SCADA) system, which has a sampling rate of approximately one sample per 4 seconds. This sampling rate is below the MC maximum duration as well as the TN fault clearing time, which in some cases within 0.042 seconds [22], [23]. The lack of capturing high-speed data samples results in poor system visibility that hinders a complete analysis of the behavior of inverter-based resources as well as DN loads during fault events. Such visibility will facilitate the understanding of DER responses in local-EPS, area-EPS, or wide area network [23].

On the other hand, the installation of phasor measurement units (PMUs) on the TN, supports system planning and operations by improving modeling accuracy and system reliability [24]. As compared with the SCADA systems, PMUs can provide the following, i) a higher degree of time granularity in terms of number of samples per second (50-60 sample per second) and higher data resolutions, ii) a fast communication access for real-time/close to real-time, iii) the capability of larger number of devices across the network, and iv) more accurate time synchronization of the measurements. Therefore, the deployment of PMUs that report to phasor data concentrators (PDCs), with a high time-stamp resolution, provides system visibility enhancement much greater than that provided by SCADA. While PMUs have been employed effectively in the past decade in the TNs, their deployment in the DNs has been very limited mainly due to their cost and the requirement for measurements accuracy for the small angles in the DNs. However, with the development of the high-precision micro-PMUs (μPMUs), the technology started to emerge in the distribution networks opening new opportunities for applications. Therefore, upgrading the DN with μPMUs, can provide valuable insight, especially as the load becomes more complex and SI-DERs reach higher levels of penetration. (Note, in the rest of the paper, the acronyms PMUs and μPMUs have been used interchangeably). It is reported in [24], [25] that PMUs represent a key equipment that can address emerging distribution system challenges and represent promising applications in different areas. These applications include planning and modeling associated with high SI-DERs penetration, system reconfiguration and power restoration, fault detection and island operation, and detection and measurement of FIDVR. In view of this, the main motivations of the paper are:

1. Although some of the literature suggested disabling the MC function in the smart inverters, the authors investigated the potential for a better management of the MC function through exploring the following questions. Does upgrading the smartness level of DER inverters to develop a response based on a global system information rather than terminal information as well as developing a dynamic setting outside the continuous operation region would enhance the operation of SI-DER and the MC function triggering? Does the integration of the μPMUs at the SI-DER level and PDC at the system level provide a better management of the MC function (rather than disabling it), and enhance the operation of distribution/transmission networks?
2. It has been reported in [16] that FIDVR events generate persistent low voltage profiles at DN leading to loss of DER generation. This raises a question about the impact of disabling MC function on the voltage profile for RAC loads and FIDVRs. Hence during faults at bulk EPS, area EPS or local EPS, does the voltage profile more sensitive to loss of SI-DERs currents due to disabling MC functions or more sensitive to voltage drop due to TN upstream currents.
3. Furthermore, in case of distribution feeders (area EPS or local EPS), how the upstream source current at the main substation (and consequently the overcurrent protection in place) can be significantly impacted by the operation of the MC in case of FIDVR events. Does triggering the MC function of multiple inverters due to faults result in no fault contributions from those inverters which leads to increasing the current at the main substation and hence impacting the whole healthy area EPS? How does the fault location (bulk EPS, area EPS or local EPS) and

disabling/enabling the MC function in smart inverters impact the main substation current and result in malfunction of the overcurrent protection?

In line with the above motivations, the main contributions of the paper can be summarized in the following.

1. The paper proposes upgrading the SI-DERs and the local-EPS aggregated loads with synchrophasor measurements. This upgrading is utilized to localize different TN/DN transient events and control the SI-DERs settings (disable/enable the MC function) during the transient event to avoid system stability issues.
2. The paper upgraded the SI-DERs response to voltage variation to be based on the system condition at the local-EPS, area-EPS, or bulk-EPS and not only at the local terminals (voltage/frequency condition).
3. The paper developed a new dynamic zone that defines the SI-DER active power delivery and reactive power exchange voltage relationship during a system transient condition (Volt-Var and Volt-Watt settings). The dynamic zone and fault localization are integrated to control (disable/enable) the MC function for different SI-DERs at local-EPS or area-EPS that are subjected to severe voltage variation.
4. The paper proposed an algorithm that enables the MC function of all SI-DERs connected in a local-EPS whenever a fault takes place within the same local-EPS. While the algorithm disables the MC function of the same SI-DERs whenever a fault takes place in the area-EPS or bulk-EPS. The advantage of adopting such a switching approach (rather than disabling the MC for all inverters) is to allow an adaptive response of the inverters (in the DN) based on the network condition which improves the system integrity. While disabling the MC function is the most appropriate for fault on the bulk-EPS for stability reasons, enabling the MC can be desirable in case of faults on the local-EPS. In this case, the MC will prevent inverters to contribute to the fault for safety reasons, as well as it allows rapid restoration of the active/reactive power in case of temporary faults to support the grid in events such as FIDVR. Enabling the MC in this case also allows the maximization of the feeder's source current in case of faults in a local-EPS feeder which facilitates the rapid isolation of the fault.

The proposed upgrading improves the voltage delay recovery due to RAC loads, enhances the SI-DERs' continuous operation, and reduces the number of lost DERs. It also provides decouple of the DN/TN protection and grid stability. For investigations, the paper also developed a measurement-based load model of the dynamic behavior of areas with high penetration residential air conditioners and investigated the impact of such loads on driving SI-DERs into MC/trip operation. The paper measurement-based simulated results show that controlling the MC function and using the proposed Volt-Var and Volt-Watt settings have enhanced the reliability of the system. The contribution of the SI-DERs currents whenever disabling MC is also monitored and shows no significant currents are detected. These results are investigated during permanent and temporary faults that take place at a local-EPS, an adjacent to local-EPS, area-EPS, or bulk-EPS. The paper proposed ultra-reliable low-latency communication (URLLC) standard provided by the new fifth generation of mobile networks (5G). The capability of 5G communication to coordinate PMU/PDC latency stages, very high peak data rates, a massive number of PMU devices, packet loss rate as well as network reliability are discussed. While the magnitudes of voltages and/or frequency variations are essential in assuring SI-DERs' continuous operation, this paper focuses on voltage variations and ignores frequency variations. This is because all data used to model the loads and sources have insignificant frequency variation that does not drive DER operation to be outside the continuous operation zone.

2. Network and Inverter Modeling

2.1. Network modeling with dynamic loads

The network model in this study is illustrated in Fig. 1, which shows a typical DN with local-EPS and high penetrations of DERs. The local-EPS consists of three main feeders: DN feeder (under monitoring and investigation), adjacent feeder, and other feeders. The DN feeder is considered the main (local) feeder in this study. It includes five busbars with their aggregated loads and two utility-scale DERs located at buses 2 and 5. The local-EPS is modeled to operate as either a radial or a ring system. Significant parts of the loads are modeled as RAC type that provokes FIDVR events during the abnormal condition. Based on the IEEE std. 1547, each local-EPS is classified under category B during normal operation which is featured with high penetrations of DERs that are subjected to frequent large variations in their output power. During abnormal operation, category III of the standard is considered that provides the highest disturbance ride-through capabilities.

A measurement-based approach is used to model the loads during the abnormal operating condition. These measurements are obtained to reflect real-time dynamic behaviors of loads during disturbances due to faults at TN and DN. The dynamic nature of the load data is collected from field measurements as reported in [21]. According to [21], the loads that have been used in their measurements contain about 70% RACs. In this study, the voltage, frequency, and active and reactive power measurements are utilized to develop and simulate the steady-state and dynamic loads which are used to investigate the response of SI-DERs and the DN during abnormal conditions. The implemented load model maps the system loads into local areas power systems (local-EPS) as defined in IEEE std. 1547. The voltage variation during transient events, as monitored at the distribution substation, the active and reactive power responses of the loads due to RACs stall and/or DERs MC/disconnection are used to simulate a dynamic load response in the PSCAD/EMTD environment. The variations in these loads are used to investigate the SI-DERs operation modes with reference to IEEE std. 1547.

As shown in Fig. 1, in the modeled local-EPS, PMUs are assumed available at the SI-DERs, the substation, and the aggregated load buses. The PMUs are used to control the SI-DERs and report the voltage and current synchrophasor measurements to PDCs located at the distribution substations. The deployed PDCs at DN and TN-PDCs are integrated and used to enhance the coupling data between the TN and DN networks. The deployment of PMUs and PDCs provides more system visibility that supports system operators of both TN and DN networks. The PMUs are utilized in this paper to monitor the variations in voltage, currents, and frequency. The voltages and currents are monitored, and their phasor representation is extracted as

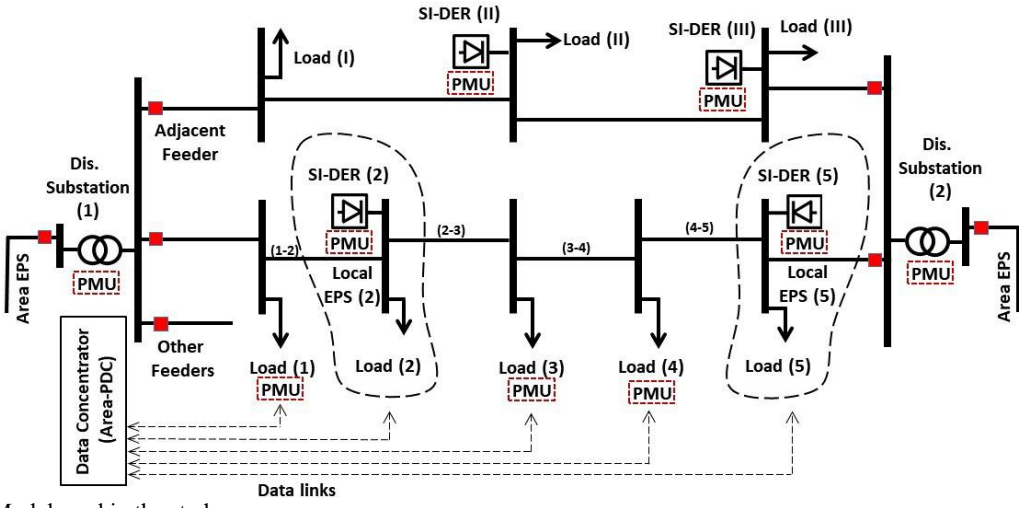

Fig. 1. DN Model used in the study.

$$v_k(t) = \frac{V_k}{\sqrt{2}} e^{j(2\pi f_o t + \delta_k)} \quad \text{and} \quad i_k(t) = \frac{I_k}{\sqrt{2}} e^{j(2\pi f_o t + \theta_k)} \tag{1}$$

where v_k and i_k are the voltage and current phasors at bus k respectively, V_k and I_k are the voltage and current magnitudes respectively, f_o is the nominal frequency and the angles δ_k and θ_k represent the phase shift of the voltage and current signals, respectively, at bus k with respect to a time-synchronized common reference. The frequency for every signal is defined as

$$f(t) = f_o + \Delta f(t) \tag{2}$$

where $\Delta f(t)$ is the deviation of frequency from nominal value and the rate of change of frequency (ROCOF) is

$$\text{ROCOF} = \frac{d}{dt} f(t) = \frac{d}{dt}\left(\Delta f(t)\right) = \frac{d^2}{dt^2}\left(\frac{\delta(t)}{2\pi}\right) \tag{3}$$

As stated earlier, however, the frequency variations and ROCOF are not shown in this study.

Fig. 2 illustrates the accuracy of the load modeling data as reported to PDCs. The aggregated loads on the five buses of a DN feeder under study and the distribution substation total load are shown in Fig. 2. These loads are

simulated and monitored during steady-state (up to 3.0 seconds) and their dynamic behavior (after 3.0 seconds) due to FIDVR events of the system shown in Fig. 1. The accuracy of the load model is validated by comparing the measurement-based simulated MW and Mvar loads extracted from [21] (dotted lines) and the PMUs data as extracted from the PSCAD simulated model (solid lines). The dotted lines of the measured data and the solid lines the PMUs reported data to the PDC show a close match of the load model. The purpose of this comparison is to validate that the load dynamics during a FIDVR event as measured by the PMUs is similar to the measurement-based load from [21]. It is important in this study that the dynamics captured by the PMUs reflect the practical response of the load. This is necessary as those responses are used to investigate the response of the SI-DER to those dynamics. It should be noted that both active power and reactive power of the load have been modeled to have the same profile based on the measurements in [21].

Fig. 3 shows the simulated voltages of five buses on a typical distribution system during two faults [21]. A temporary TN fault (Fig. 3a), which is cleared very fast (within 3 cycles), yet affected a large area of the DN healthy feeders [17]. The impact of this fault has been seen as a sudden reduction in the voltages at the DN buses. Due to the RAC loads, a FIDVR was observed at the distribution level and causes a loss of a significant part of medium voltage level SI-DERs and rooftop DERs (MC and trip, $V < 0.50$ pu for $t > 1.0$ second). The case in Fig. 3a, the FIDVR at one of the healthy DN feeders that lasts for 27 seconds before returning the voltage to normal values. The second fault is a temporary fault (Fig. 3b) on a segment of a DN feeder. This fault shows a FIDVR that lasts for 12 seconds before restoring voltages to all buses at the DN feeder. Fault impedances used in these investigations varied from 0.5-10 Ω.

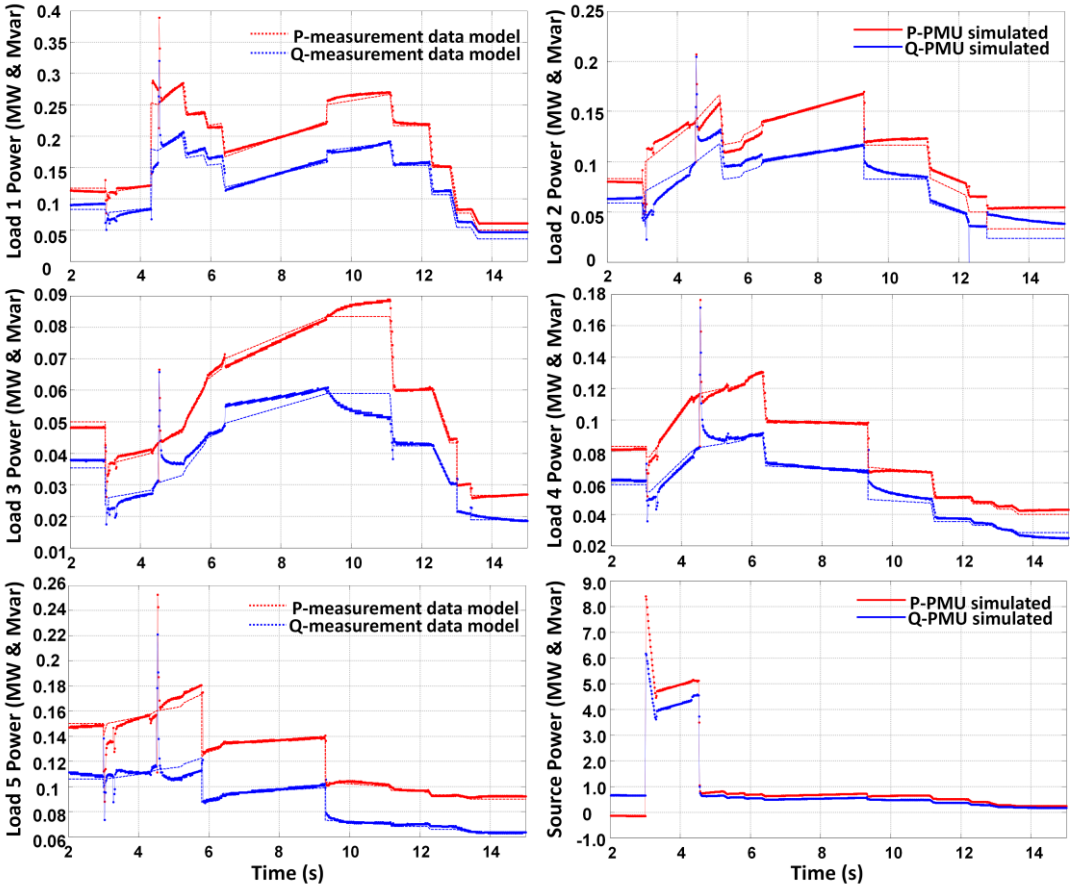

Fig. 2. The steady-state and dynamic behavior of the DN feeder's loads and source power during a fault event.

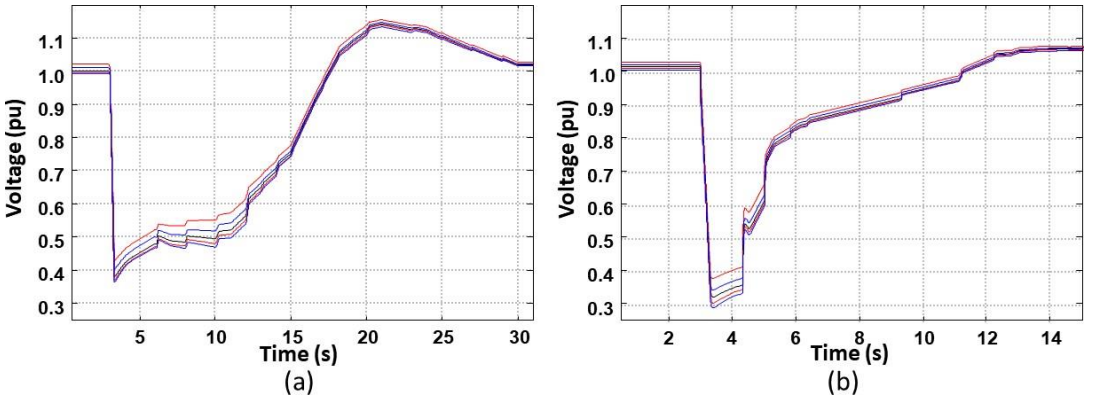

Fig. 3. FIDVR at distribution system due to a) fault at transmission level and b) fault at distribution system.

During these events, whether the fault is at TN or a segment of a DN feeder, voltage sags cause the RAC units to stall and drive SI-DERs to MC that cease current injection and trip (if the terminal low-voltage persists beyond the threshold time defined in the IEEE 1547 std.). This leads to an increase in loads (seen by the source substation) and a loss of DERs generation. Consequently, more current is supplied from the grid feeder that activates the protection relays and disconnects customers and generators at DN feeders regardless faults are temporary, fast cleared at TN, or at a segment of DN feeder. Both of the events in Fig. 3 represent a challenge to distribution system protection, the SI-DERs ride-through, and continuous operation as well as the stability of TN.

2.2. Inverter modeling and management

An electromagnet transient (EMT) based model has been used in this study to accurately capture the transient/dynamic responses of the inverters during contingencies. The inverter model used in the simulations is the detailed model of a two-level, three-phase voltage source inverter (VSI) simulated in PSCAD (using discrete switch models). The inverter is controlled mainly to regulate the active and reactive power using vector control in the *dq*-frame and standard PI compensators as illustrated in Fig 4.

As illustrated in Fig. 4, the inverters are managed with the PMUs and PDCs. The PDCs process the reported PMUs data and define system normal/abnormal condition. The PMU data reporting (voltage and current of synchrophasors, frequency, and ROCOF measurements) is arranged to cover 10-120 frames per second (fps) for 60Hz system (10-100 fps for 50Hz system) [26] based on the real-time (or close to real-time) requirement of the system response. The communication interface requirement of the SI-DER ($\leq$ 30 seconds, [9]) should be updated to match PMU applications. The communication method between the PMUs and the PDCs should consider the SI-DER locations and available communication infrastructure to develop a real-time application. Analyzing the data of the PMUs allows the PDCs to control SI-DERs and define fault location, update their functions, as well as isolate faulty feeders and restore power to healthy EPS- areas. The PDC also reports the processing results to the main control station, hence the DN/TN PDCs are integrated to overcome TN-DN decoupling and provide control commands to the SI- DERs PMUs that reflect the system condition and not only DERs terminal condition.

During normal operation, the DN-PDC is used to manage the reference values of the active and reactive power (P and Q set values). During the abnormal condition, the PDCs define fault location and control the smart inverters' dynamic performance by enabling/disabling the MC function and other SI-DERs modes. Thus, in the implemented controller, the set values of the active and reactive power are constantly managed in close to real-time to proactively support the grid operation. The current limit logic in the local controller ensures inverter currents do not exceed the maximum (rated) current of the inverter. The details of the proposed set values during the normal and abnormal conditions are described in section 4.

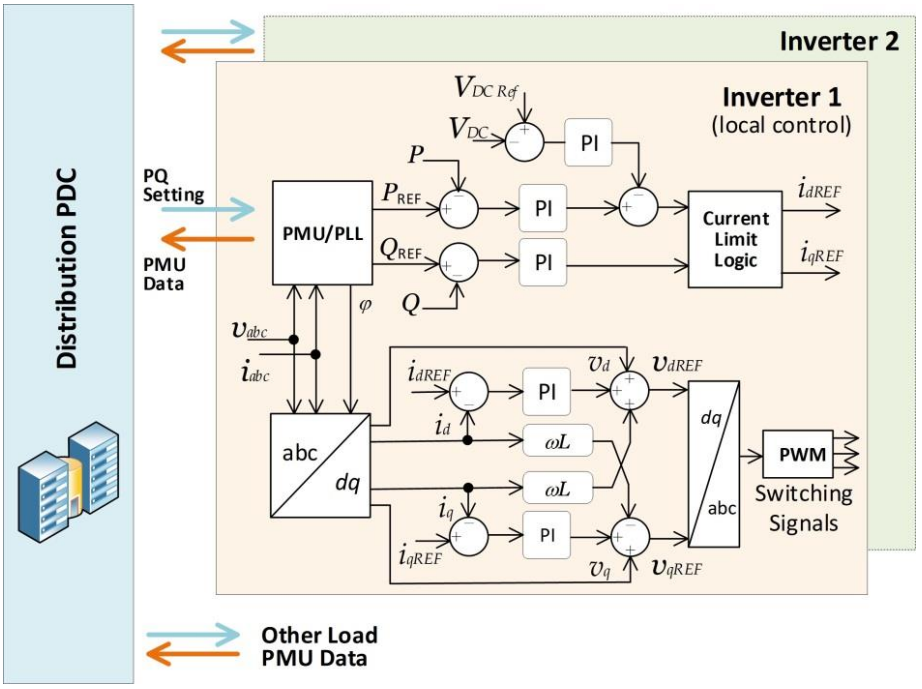

Fig. 4. Inverter local control and its integration with PMU and PDC.

The accuracy of the responses of the inverter's control is evaluated by comparing the inverter's output active and reactive powers based on the set values extracted from IEEE std. 1547 (volt-var and volt-watt operation modes) and the inverter output powers as extracted using the PMUs. Fig. 5 compares the set values P_{inv}^{set} and Q_{inv}^{set} (blue plots) of the inverter that is connected to bus 5 as well as its PMU measured values P_{inv}^{meas} and Q_{inv}^{meas} (red plots) during a fault. The result of the figure depicts the accuracy of the model response as compared to the PMU measured data. It should be noted that, the inverter ride-through response is affected by the fault duration period as well as the RAC loads response due to voltage variation which is extended beyond the fault duration period.

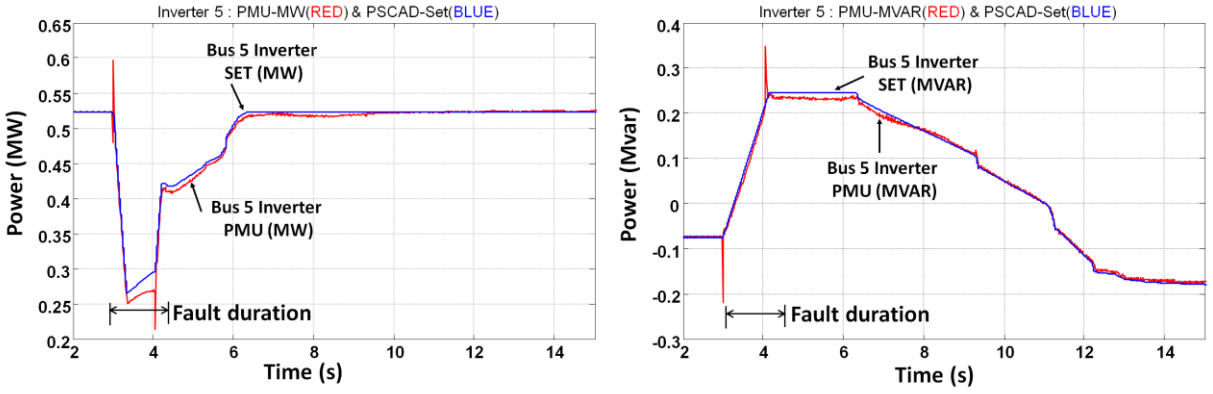

Fig. 5. Inverter P and Q set values and PMU extracted values during inverter ride-through response to a fault.

3. Impact of the Abnormal Operation on the Distribution and Transmission Networks

The collective impact of transient events on DN feeder and SI-DERs as well as the grid power is investigated in this section. Different cases of temporary and permanent faults on DN and TN are considered in this paper. These investigations are aimed to underline that, despite the different locations or the different nature (temporary or permanent) of the events, they can drive different inverters at different parts in the network, simultaneously, to the same operation mode (whether it is momentary cessation, ride-through, or trip). This is mainly because inverters respond only to local measurements.

Fig. 6 shows the responses of the two inverters connected to the DN feeder understudy (in Fig. 1) due to faults on the TN, DN adjacent feeders, and the DN feeder under study. The figure illustrates five case scenarios arranged in five columns. Each case shows the PMUs extracted voltages on each bus (V_2, V_5) and the active and reactive power of bus 2 and bus 5 inverters (P_{inv}^{meas} and Q_{inv}^{meas}), and the grid current ($Isource$) at the distribution substation.

Case 1 (Fig. 6, column 1) shows the impact of a FIDVR in the DN feeder due to a temporary transient event (balanced fault) on the TN. This event generated a DN-FIDVR that drives the SI-DERs to the following operation modes:

- Inverter 5 on bus 5 enters the MC mode shortly after the fault occurred and recovered in less than 1s (V_5 <0.5pu).
- Inverter 2 on bus 2 rides through the event (V_2 >0.5pu).

Case 2 (Fig. 6, column 2) presents another temporary fault on the TN causing a deeper voltage drop on the DN which drives the two inverters on the DN to the following.

- Both inverters 2 and 5 enter the MC mode soon after the occurrence of the fault (V_5 <0.5 and V_2 <0.5).
- Inverter 5 trips as the voltage dip lasted for more than1s, while inverter 2 recovers within 1s.
- Inverter 2 enters the MC mode again due to a voltage increase at the end of the FIDVR event (V_2 >1.1pu) before it trips.

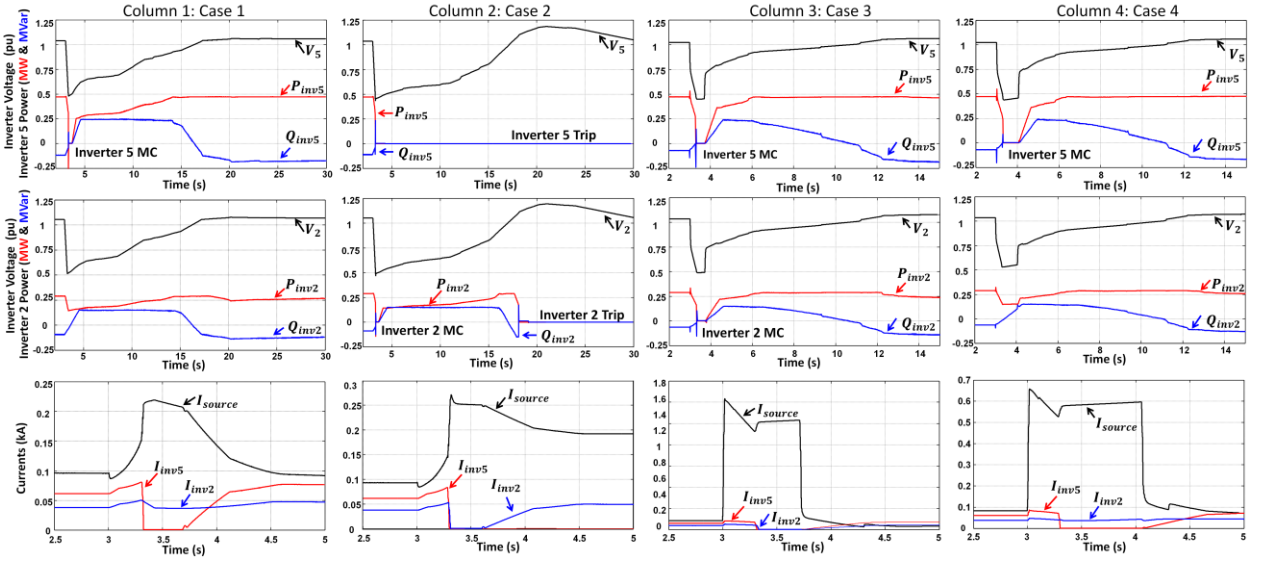

Fig. 6. The DN grid and inverters power during TN and DN transient events.

Case 3 (Fig. 6, column 3) illustrates fault event occurred at an adjacent feeder to the DN feeder understudy. The event caused the following modes:

- Both inverters 2 and 5 enter the MC mode soon after the occurrence of the fault.
- Both inverters recover within 1s.

Case 4 (Fig. 6, column 4) shows an event due to a fault on the DN feeder at the feeder section 3-4. The fault was self-cleared after 0.35s. This event triggers the following:

- Inverter 2 rides through the event (V2>0.5pu).
- Inverter 5 enters the MC mode before recovers within 1s.

In all of the investigations, the following remarks can be concluded.

- In all cases, it can be observed that the main substation current (I_{source}) increases significantly when one or more inverters enter the MC mode. This current increase is due to the system response to the dynamic behavior of the load due to FIDVR events and the lost power of the inverters (seize to energize due to MC). This lost power is supplied from the TN and becomes significant if a wide area in the DN is affected by the FIDVR as the case in the TN faults. While this increase is desirable in the case of faults on the DN causing fast protection reaction, it is not the case for faults outside the DN as they cause a false operation of the protection systems.
- In cases 1-3, despite the faults were outside the DN feeder, the inverters on the healthy feeder entered the MC mode for several intervals.
- Loads on the DN exhibited dynamic prolonged responseseven to transient faults on TN. This response can be observed from the variations in I_{source} in the bottom plots in Fig. 6. This can be also observed from the wide variations in active and reactive power responses in Fig 2. This dynamic response is exaggerated by the loss of the after-the-meter (rooftop small inverters) and the FIDVR. This underlines the coupling between the TN and DN.

Therefore, for operational improvement, during these events, the SI-DERs' response should be categorized and controlled such that their response is controlled not only based on the terminal voltage and frequency profile. The SI-DERs response should consider a wide area system condition and not only the condition at the connection terminals. The information about the event type, location, and the dynamic nature of the local-EPS load (FIDVR) as well as the loss of the after-the-meter rooftop DERs should be considered. The impact of the SIs operation mode, active and reactive power priority, and functions should also be considered. Such control should support the TN stability, the DN reliability, and end-users quality of services during faults at wide area network, area-EPS, or local-EPS. Based on the area-EPS and local-EPS, the SI-DERs should be able to delay and adjust MC duration settings, disable/enable these functions, and/or change the SI-DERs operation mode. This can be achieved by overriding the decouple operation and allowing wide-area system condition information sharing among the TN/DN operators in real-time.

4. The proposed algorithm

The increased visibility of DN power flows and bus voltages in real-time can increase the capability to grid control and analyses based on the PMU real-time data. In the proposed system, all buses appear as autonomous nodes that develop an event-driven network capable of reporting-by-exception whenever the monitored features are upgraded from a state to another. This real-time observability supports real-time assessment for protection and control and fast decision-making for the DSO in defining system state and DERs status. Furthermore, the achieved observability enhances the DSO competence to diagnose the equipment health condition, detect and anticipate early stages of impending faults and equipment failure. It also provides a means to analyze an event post disturbance for situation awareness and effective managing and optimizing DER resources, as well as continuous updating of system models. The following subsections describe the proposed approach to upgrade the DER operations and improve the system visibility.

4.1. Proposed Upgrading Settings of the Managing Entity (DER-MME)

The local DER setting is upgraded in this paper to include the DER-SIs operation outside the steady-state continuous operation mode as defined in the IEEE std. 1547-2018. For example, the decision of disabling/enabling MC operation, during transient events, is proposed to be performed within a limited time while the applicable voltage or the system frequency is outside the continuous operation mode. It is worth it to mention that this paper is focused on upgrading the momentary cessation operation setting based on only the voltage variations, assuming the applicable frequency is within specified continuous operation parameters. The SI-DERs functional and setting update is performed smoothly and without developing transients at the DER outputs.

The paper proposes a "continuous to energize" dynamic setting zone that can be utilized whenever the MC mode is disabled. The proposed zone defines the DER active power delivery and reactive power exchange during a system transient condition that drives the voltage variation towards MC operation. Fig. 7 shows the upgraded volt/var and volt/watt droop settings of the inverters. The inverter output power outside the voltage range defined in the IEEE std. 1547, is proposed by extending the voltage/power output relationship outside the continuous operation mode. It should be highlighted that, while the IEEE std. requires the inverter to enter an MC mode if the voltage drops below 0.5 pu, (i.e., P= 0 and Q= 0), in this paper, it is proposed that the volt/var and volt/watt relationships are extended (by the blue and red lines) to develop a dynamic setting zone that allows DER-SIs to generate power outside the continuous operation zone. This dynamic zone covers the SI response when voltages are below low voltage or high voltage MC mode ($V < V_L \; or \; V > V_H$) and whenever the MC mode is disabled by the PDC. For purpose of this study, a reactive power priority (Q-priority) mode has been considered to provide maximum reactive power support in case of the FIDVR events. In this mode, the reactive power is set based on the volt/var curve and used to calculate the reactive current set-value. The active current is then calculated based on the rated current of the inverters. This is illustrated by (4) and (5).

$$I_{qREF} = \frac{Q_{REF}}{|V|} \tag{4}$$

$$I_{dREF} = \sqrt{I_N^2 - I_{qREF}^2} \tag{5}$$

where I_{qREF} and I_{dREF} are the quadrature and direct components of the inverter current (as they indicated in the current logic in Fig. 4), $|V|$ is inverter terminal line voltage, and I_N is the inverter rated current. As previously mentioned, the proposed algorithm in this paper considers insignificant frequency variation in the DN during different events and focuses only on voltage variations.

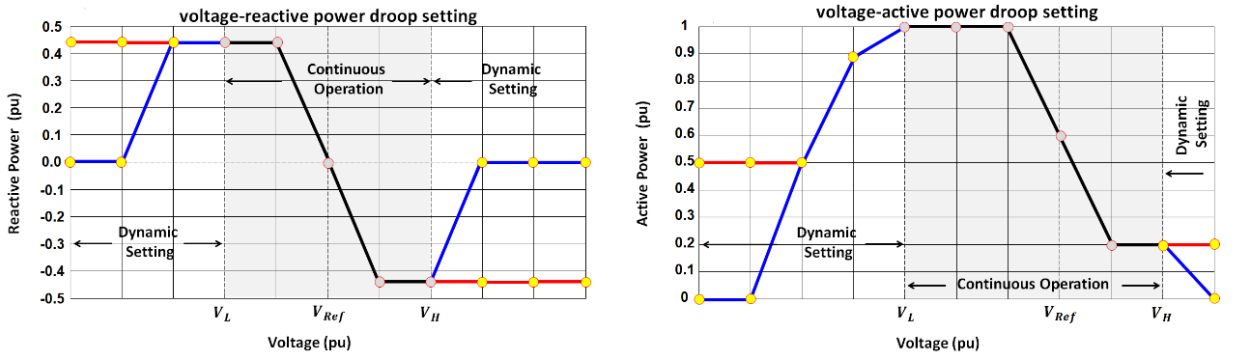

Fig. 7. The existing "continuous operation" and the proposed "dynamic setting" volt/var and volt/watt droop responses of the inverters.

Fig. 8 illustrates a high-level structure of the proposed DER-MME. The figure depicts the monitoring and managing links proposed to upgrade the SI-DER control and management and thus, providing the means to de-couple the DN/TN operation. The normal and abnormal operating conditions are monitored and defined by processing the real-time synchronized PMUs data as reported to PDC at the distribution substation. Based on the network operating condition overseen by the Area-PDC, the appropriate operating mode (or activating/deactivating functions) of the SI-DER can be activated. Accordingly, the reference active and reactive powers (P_{REF} and Q_{REF}) are identified in the inverter local control in accordance with the settings defined in IEEE std. 1547 as well as the proposed zone whenever the operation is outside the continuous zone (in the dynamic zone) as illustrated in Fig. 7.

It is pertinent to mention that, while the proposed DER-MME is a general monitoring and managing approach for all inverter functions/modes, this study focused specifically on implementing the DER-MME for enabling/disabling the MC mode for dynamic support of the voltage profile. The decision to activate/deactivate the MC function is based on a proposed fault detection and localization algorithm which is described in section 4.3.

4.2. Communication Challenges of the Managing Entity (DER- MME)

The data quality and communication requirements are the main challenges for the applications of DER-MME in a modern and smart distribution system with a variety of energy resources and RAC loads. The proposed DER-MME is relying on a communication network between area PMU-PDC and multiple PMUs in order to monitor and manage the operation of different DERs. The area PMU-PDC processes the time-synchronized phasor measurements as reported from the area and local SI-DERs and aggregated loads. The results are used to define in real-time the operation condition in the local/area EPS and updated SI-DERs functional and mode settings accordingly. All aggregated measurements are tagged with the UTC time through the Global Positioning System (GPS). The upgraded DER-MME structure and its communication capability are developed to match PMUs data exchange for real-time application.

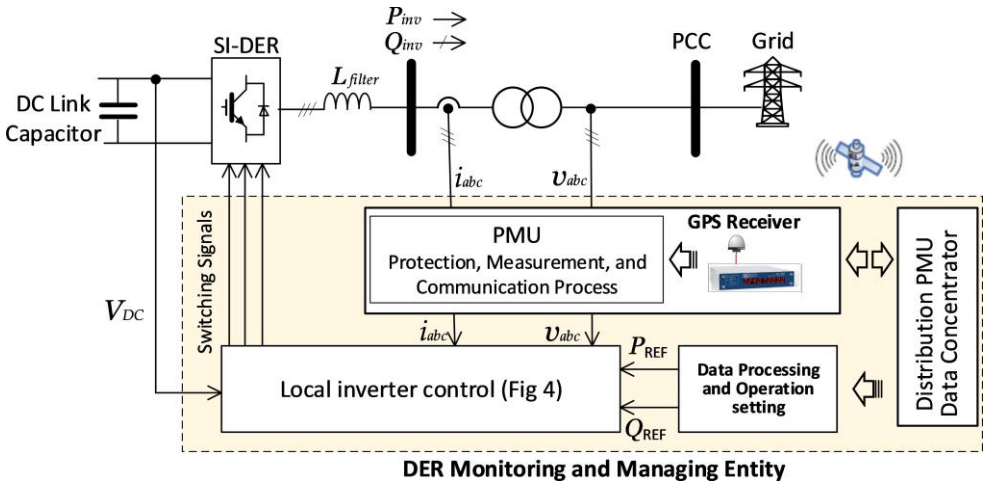

Fig. 8. Structure of the proposed DER-MME.

Based on the available communication technologies, we propose the integration of ultra-reliable low-latency communication (URLLC) standard provided by the new fifth generation of mobile networks (5G). The URLLC is one of the most significant developments to the 5G network standard and is directed mainly for industrial applications. It can achieve 99.999% reliability with user-plan and control plan latencies of 1 ms and 10 ms respectively [**27**]. The 5G is around 100 times faster than existing mobile technology (4G) with a transfer rate of 20 Gbps [28]. This new technology provides connections with very high peak data rates that supports mobile broadband (eMBB). It also provides machine-type communications (mMTC) that supports a massive number of PMU devices with a less than 1% of packet loss rate [29]. Based on the communication requirements of intensive distributed PMUs to provide their data over long-range and within a restrictive time, it looks that the 5G-based URLLC is the natural communication-technology best candidate at the moment. The 5G communication has the capability to coordinate DER-MME latency stages that include PMU computation and processing window, network delay, PDC processing delay, and the control process delay. It has been reported in [**30**], data measured by PMUs can transmit to a control center every 0.01s via a 5G network however, DER-MME processing and control action delay present an additional latency. Data loss due to GPS signal loss or communication network congestion is dropped by a time-out function that is linked with the time-stamp of the reported data. Furthermore, as reported in [31], the accuracy of PMU-based fault detection and localization is directly related to the implemented sampling rate of the current and voltage signals and a time resolution of at least 1/50 of a second (50 Hz system) and a corresponding time error of 100 μs is required. The IEEE std. C37-118 [32] encourages higher data rates, such as 120 frames/s, that enhances the accuracy, however adding a computational margin. The estimated values of the latency and data rates in the literature are based on simulation and (or) laboratory application and implementation in a real power system as well as security assurance still present a challenging task.

In general, faults that generate slow-time voltage sag towards MC mode (less than 0.5 pu) are more practical to accommodate in real-time application of the control response and disable/enable MC functions. For example, in Fig. 3b there are 15 cycles (PMU data rates up to 30 frames) before the bus voltage reach 0.5 pu. However, faults that generate instantaneous voltage sag to less than 0.5 pu (Fig. 3a) present a great challenge for real-time application. A predefined time delay should be considered in such cases before activating the MC function in order for the proposed algorithm to define the fault-location and hence enable/disable the MC function.

4.3. Fault Detection and Localization Algorithm

The goal of the proposed algorithm is to allow a dynamic MC response of SI-DERs during abnormal transient events that impact voltages such as FIDVR. During a transient event at TN or DN, a FIDVR is propagated at the DN and the SI-DERs detect voltage reduction that impacts their continuous operation. Furthermore, the distribution protection system detects high currents that might disconnect the feeders. Due to the increasing coupling between the TN and DN, the response of SI-DERs and the protection system should be hinged to fault location (DN/TN faults) and not only to the developed FIDVR. Defining the source of a transient event allows DSO to coordinate with TSO to take prompt action to secure the reliable and continuous operation of SI-DERs.

The proposed fault detection and localization algorithm integrates the impedance estimation fault detection method and multi-terminal measurement method. The algorithm assumes the availability of the time-synchronized measurements (TSMs) of voltage and currents at SI-DERs and load buses. In addition, it assumes TSMs can be extracted from PMUs at the IEDs in primary substations and outgoing feeders. The multi-terminal measurement method is incorporated by using the TSMs to estimate, in real-time, the feeder currents in forward (I_{FOR}) and backward (I_{BACK}) directions.

During normal operation conditions (NOC), the estimated time-synchronized value of the forward direction current $[I_{FOR}]_{pq}^{NOC}$ between two buses p and q is

$$[I_{FOR}]_{pq}^{NOC} = \begin{cases} I_{si} & i = 1 \\ I_{(i-1)i} + I_{DERi} - I_{Li} & i = 2:(k-1) \end{cases} \tag{6}$$

where I_{si} $(i = 1)$ is the TSM of the current supplied from the primary substation in the forward direction and I_{DERi} is the SI-DER current at bus i. The total number of buses in the feeder is k. Similarly, the backward direction current $[I_{BACK}]_{pq}^{NOC}$ between any two buses is

$$[I_{BACK}]_{pq}^{NOC} = \begin{cases} I_{kS} & i = k \\ I_{(i-1)i} + I_{DERi} - I_{Li} & i = (k-1):2 \end{cases} \tag{7}$$

where I_{kS} is the measured synchrophasor current supplied from bus k towards the primary substation. During normal operation condition, both forward and backward monitored synchrophasor currents are approximately equal as follows.

$$[I_{FOR}]_{pq}^{NOC} = [I_{BACK}]_{pq}^{NOC} \tag{8}$$

To incorporate the impedance estimation method, the feeder segment catalog impedances (from manufacture) and the TSMs of the voltages at each bus are used to calculate the currents $[I_{CAL}]^{\mathrm{NOC}}$ in each feeder segment.

$$[I_{CAL}]_{pq}^{NOC} = |I_{i(i+1)}|^{\angle\delta_{i(i+1)}} = \frac{|V_i|^{\angle\theta_i} - |V_{i+1}|^{\angle\theta_{i+1}}}{\left|Z_{i(i+1)}\right|^{\angle\beta_{i(i+1)}}} \tag{9}$$

where V_i is the measured synchrophasor voltage at bus I, and $Z_{i(i+1)}$ is the feeder segment impedance as defined by the feeder's manufacture.

During a fault condition, the forward direction current $[I_{FOR}]_{pq}^{F}$ and $[I_{BACK}]_{pq}^{F}$ are used to estimate the current at any feeder segment of the faulty feeder. The primary substation feeder segment current is based on the substation PMU measurement. The calculated currents $[I_{CAL}]_{pq}^{F}$ can correctly estimate the currents in all feeder sections except the faulty section. This is due to the change in the impedance of the faulty section as a result of the fault impedance.

A feature matrix is used to define the faulty segment in a feeder. This matrix is developed based on the impedance estimation fault detection method and multi-terminal measurement method. When a fault or transient event takes place in any feeder section of a radial/meshed distribution system, the faulty feeder segment location is defined as

$$[\text{Faulty Segment}]_{pq} = [\Delta M]_{FOR} \cdot [\Delta M]_{BACK} \neq 0 \tag{10}$$

where $[\Delta M]_{FOR}$ and $[\Delta M]_{BACK}$ are feature matrices and ϵ represents the error between the impedance estimation fault detection method and multi-terminal measurement method which are calculated as follows

$$\begin{aligned} [\Delta M]_{FOR} &= \left|[I_{CAL}]_{pq}^{F}\right| - \left|[I_{FOR}]_{pq}^{F}\right| \\ \&\ \ [\Delta M]_{FOR} &= 0 \quad \text{if} \quad [\Delta M]_{FOR} < \epsilon \end{aligned} \tag{11}$$

$$\begin{aligned} [\Delta M]_{BACK} &= \left|[I_{CAL}]_{pq}^{F}\right| - \left|[I_{BACK}]_{pq}^{F}\right| \\ \&\ \ [\Delta M]_{BACK} &= 0 \quad \text{if} \quad [\Delta M]_{BACK} < \epsilon \end{aligned} \tag{12}$$

Those feature matrices are used by the DER-MME to identify the condition of the network and manage the SI-DER accordingly. This is illustrated in the following results sections.

5. Results and discussion

5.1. Validation of the Fault Detection and Localization Technique

The fault detection and localization technique has been tested and validated on numerous fault cases applied at different locations, durations, and fault impedance on the test network in Fig. 1. Some of the results are presented in Fig. 9 which shows the feature matrices of all the segments of the distribution feeder for different fault scenarios. The feature matrices presented in Figs 9(a) to 9(d) are for faults outside the DN feeder (either on the TN or on the adjacent feeders of Fig. 1), whereas Fig. 9(e and f) shows the feature matrix in case of a fault is located in the DN feeder under study. Figs 9(a, b, c and d) are the feature matrices for TN/DN events defined by cases 1-3 in Fig. 6. Fig 9(e and f) represent the feature matrix for DN event at DN feeder understudy during a fault of 0.19s at the feeder segment 2-3 and 1.05s at the feeder segment 3-4 (case 4 in Fig. 6). The figure reveals that the feature matrices can clearly detect the faulty segment and thus, identify whether the fault is within the DN feeder understudy. This is important in the proposed DER-MME in order for the SI-DER to respond accordingly.

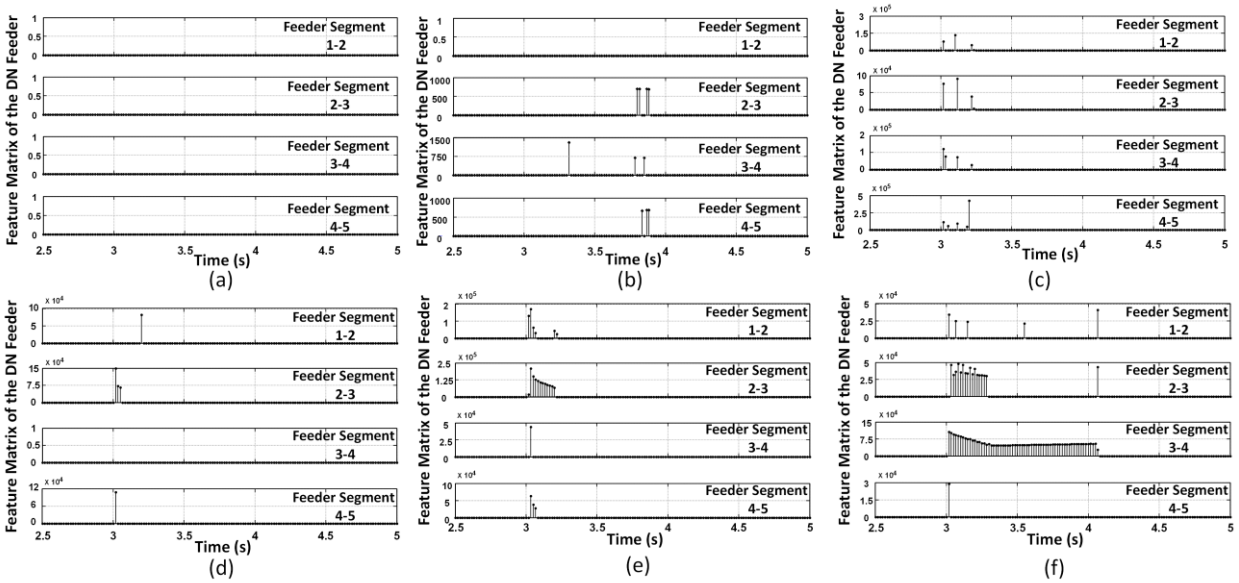

Fig. 9. Feature matrices of the DN feeder's segments in the DN in Fig. 1.

5.2. The Performance of the Proposed DER-MME for Minimizing the Impact of FIDVR Events

The DER-MME has been used to dynamically control the MC function of the SI-DER based on the fault locations. Fig. 10 shows the enhancement of the system due to the proposed DER-MME considering different FIDVR events caused by faults at TN (case 1 of Fig. 6), DN adjacent feeder (case 3, of Fig. 6), and DN local feeder (case 4, of Fig. 6). The results are based on simulations conducted on the test network shown in Fig. 1.

Fig. 10 (a) compares the results without/with the proposed DER-MME during a temporary fault on the TN that generates FIDVR on all DN buses of the feeder under study (case 1 of Fig. 6). The top two figures (of Fig. 10 (a)) compare the enhancement in the bus voltages. The bottom figure compares the two inverters and the substation currents. The dashed lines represent the currents in the base system and the solid lines represent the DER-MME based system response. For the base system, the voltage dropped at bus 2 to less than 0.5 pu and inverter 2 entered the MC mode (seize to energize, dashed red line). The system loses a potential reactive power from inverter 2 that supports the mitigation of the voltage drop. The dynamic nature of the load (RACs stall) causing large reactive power demand which leads to delayed voltage recovery. The inverter lost power is substituted from the TN causes a high substation current (***Isource***) as shown in the figure (dashed line in Fig. 10 (a)). Based on the proposed DER-MME, the feature matrix for such event (case 1 of Fig. 6 and Fig. 9(a)) indicates that the fault is outside the monitored DN feeder. The MC mode is disabled and inverter 2 provides more reactive power support based on the proposed dynamic setting of the volt/var as proposed in Fig. 8. Implementing the DER-MME enhances the voltage response as depicted in the top-right plot of Fig. 10(a) and causes a significant reduction in the substation current as shown by the solid line in the bottom plot of Fig. 10 (a). This reduction in the DN substation current restrains the impact of SI-DER MC mode and FIDVR currents on the TN, particularly in the case of wide DN areas are affected by a voltage reduction event.

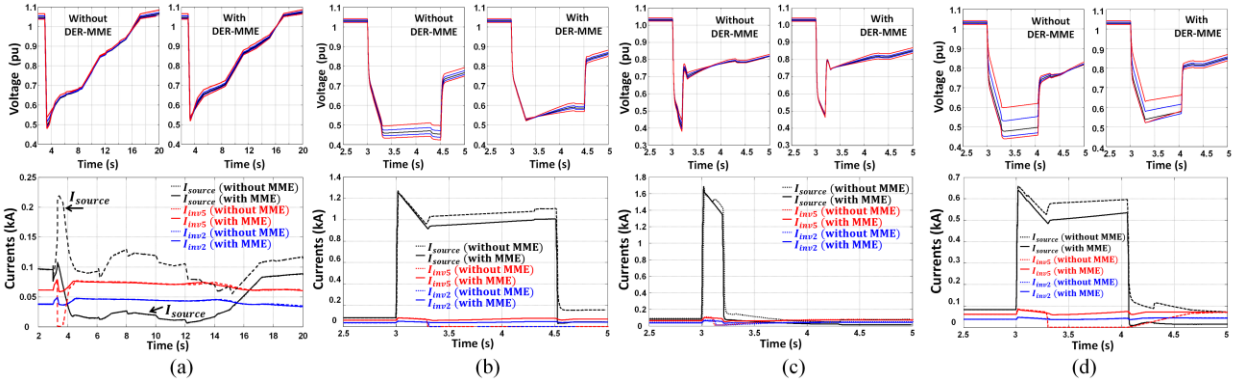

Fig. 10. Effects of DER-MME implementation to dynamically control the MC mode for minimizing the FIDVR events.

Figs. 10(b) and (c) show FIDVR cases due to permanent (cleared after 1.5s) and temporary faults respectively. Both faults occurred on the adjacent DN feeder. The proposed DER-MME shows that the fault is not in the DN feeder understudy, and MC mode is disabled. The impact of disabling the MC mode, in this case, can be seen from the clear improvement in the voltages of the DN feeder during and after the fault while the changes in the inverters and substation currents were not significant.

The last case in Fig. 10(d), presents the response for a permanent fault on line 3-4 on the local DN feeder (case 4, Fig. 6 and Fig. 9(f)). This fault caused the voltages at buses 3, 4, and 5 to drop below 0.5 pu. Since the fault was detected on the DN local feeder, the MC was enabled by the DER-MME, and as a result, the inverter at bus 5 entered the MC mode. A high substation current can be observed which causes the fault to be cleared rapidly. However, for investigating the impact of the proposed DER-MME in case of temporary faults (not permanent). The MC mode is also disabled or delayed and results are compared with the case when the MC was enabled. Disabling or delaying the MC mode enhances the voltage response as depicted in the top-right plot of Fig. 10(d). Furthermore, it causes no significant change in inverters' currents, however, it causes a reduction in the substation current (the solid line in the bottom plot of Fig. 10 (d)) which delays the protection relay response until declare a permanent (not temporary) fault.

It should be highlighted that, from the results and in terms of voltage responses during the FIDVR, despite the small recovery in the voltage profiles, supporting the voltages using the proposed DER-MME to restore the voltage above the 0.5 pu threshold was necessary to prevent several RAC loads to stall (RACs stall at 0.5 pu as explained in section 1). This consequently can reduce the impact of the FIDVR events as fewer loads will stall.

6. Conclusions

The focus of the paper has been specifically on the impact of voltage variation due to faults at TN/DN (local-EPS, area-EPS, and bulk-EPS) on the DN voltage delay recovery and MC/Trip operation of SI-DERs. Based on several investigations, it has been shown that triggering the MC function of the inverters based only on the local voltage/frequency information and the lack of visibility between the DN and TN can adversely impact the voltage profile during FIDVR events. Furthermore, MC/Trip mode increases the number of lost SI-DERs and hence impacts system stability. The paper proposed an upgrade to SI-DERs response to voltage variation to be based on the system condition at the local-EPS, area-EPS, and bulk-EPS and not only at the local terminals (voltage/frequency condition). In this paper, a monitoring and management entity (DER-MME) is proposed for dynamically managing distribution system smart inverter functions/operations during faults in TN/DN. Two upgrades are proposed on the system level and device level. At the system level, the SI-DERs and the local-EPS aggregated loads are upgraded with synchrophasor measurements that provide a way to define fault locations. At the device level, the standard settings (IEEE std 1547-2018) are upgraded by a new dynamic zone for SI-DER active/reactive power voltage relationship to provide a new setting for SI-DERs operation outside its continuous operation zone. The paper shows that implementing and controlling these two suggested upgrades by the DER-MME improves the system reliability. The proposed DER-MME enhanced the SI-DERs operation considering the area-EPS conditions and not only the voltage and frequency at the inverter terminals. The algorithm improves the voltage delay recovery due to RAC loads and hence enhances the voltage profile. It supports the SI-DERs continuous operation, delays the MC/Trip operation, and reduces the number of lost DERs due to MC/Trip functions. It also provides decouple for the DN/TN protection and stability actions.

The integration of PMUs and PDC with the SI-DER in the proposed DER-MME shows very promising results. The visibility between the DN and TN is attained and faults can be detected and localized in local-EPS or area-EPS and hence promptly control the SI- DERs functions and modes. The proposed approach was tested on a typical DN where results showed that a better voltage profile can be achieved and thus stability can be improved.

References

[1] S. Kerscher, and P. Arboleya, “The key role of aggregators in the energy transition under the latest European regulatory framework,” *International Journal of Electrical Power & Energy Systems*, vol. 134, 107361, January 2022.

[2] R. Hao, Q. Ai, Z. Jiang, and Y. Zhu, “A novel adaptive control strategy of interconnected microgrids for delay-dependent stability enhancement,” *International Journal of Electrical Power & Energy Systems*, vol. 99, pp. 566-576, 2018.

[3] F. Rohde and S. Hielscher, “Smart grids and institutional change: Emerging contestations between organisations over smart energy transitions,” *Energy Research & Social Science*, vol. 74, 2021.

[4] Y. Zhou, Z. Li, and M. Yang, “A framework of utilizing distribution power systems as reactive power prosumers for transmission power systems,” *International Journal of Electrical Power & Energy Systems*, vol. 121, 106139, 2020.

[5] R. Wallace Kenyon, B. Mather and B.-M. Hodge, “Coupled transmissionand distribution simulations to assess distributed generation response to power system faults,” *Electric Power Systems Research*, vol. 189, no. 106746, 2020.

[6] I. Alvarez-Fernandez, D. Ramasubramanian, W. Sun, A. Gaikwad, J.Boemer, S. Kerr and D. Haughton, “Impact analysis of DERs onbulk power system stability through the parameterization of aggregated DER a model for real feeders,” *Electric Power Systems Research*, vol. 189, no. 106822, 2020.

[7] M. Jalali, V. Kekatos, N. Gatsis and D. Deka, “Designing Reactive Power Control Rules for Smart Inverters Using Support Vector Machines,” *IEEE Transactions on Smart Grid*, vol. 11, no. 2, pp. 1759-1770, March2020.

[8] R. K. Varma and S. Mohan, “Mitigation of Fault Induced DelayedVoltage Recovery (FIDVR) by PV-STATCOM,” *IEEE Transactions onPower Systems*, vol. 35, no. 6, pp. 4251-4262, 2020.

[9] "IEEE Standard for Interconnection and Interoperability of Distributed Energy Resources with Associated Electric Power Systems Interfaces," *IEEE Std 1547-2018* (Revision of IEEE Std 1547-2003), 2018.

[10] R. Guttromson and M. Behnke, "Momentary Cessation: Improving Dynamic Performance and Modeling of Utility-Scale Inverter Based Resources During Grid Disturbances," No. SAND2020-0266. Sandia National Lab. (SNL-NM), Albuquerque, NM (United States), 2020.

[11] B. J. Pierre, M. E. Elkhatib and A. Hoke, "Photovoltaic Inverter Momentary Cessation: Recovery Process is Key," *2019 IEEE 46th Photovoltaic Specialists Conference (PVSC)*, 2019, pp. 1561-1565.

[12] H. Shin, J. Jung, S. Oh, K. Hur, K. Iba and B. Lee, "Evaluating the Influence of Momentary Cessation Mode in Inverter-Based Distributed Generators on Power System Transient Stability," *IEEE Transactions on Power Systems*, vol. 35, no. 2, pp. 1618-1626, 2020.

[13] S. Kang, H. Shin, G. Jang and B. Lee, "Impact analysis of recovery ramprate after momentary cessation in inverter based distributed generatorson power system transient stability," *IET Generation, Transmission & Distribution*, vol. 15, no. 1, 2021.

[14] B. J. Pierre, M. E. Elkhatib and A. Hoke, "PV Inverter Fault Response Including Momentary Cessation, Frequency-Watt, and Virtual Inertia," *in* IEEE *7th World Conference on Photovoltaic Energy Conversion(WCPEC)*, Waikoloa, HI, USA, June 2018.

[15] S. Zhu, D. Piper, D. Ramasubramanian, R. Quint, A. Isaacs and R. Bauer, "Modeling Inverter-Based Resources in Stability Studies," *2018 IEEE Power & Energy Society General Meeting (PESGM)*, 2018, pp. 1-5.

[16] R. W. Kenyon, and B. A. Mather, "Simulating distributed energy resource responses to transmission system-level faults considering IEEE 1547 performance categories on three major WECC transmission paths," No. NREL/TP-5D00-73071. National Renewable Energy Lab. (NREL), Golden, CO (United States), 2020

[17] R. W. Kenyon and B. Mather, "Quantifying Transmission Fault Voltage Influence and Its Potential Impact on Distributed Energy Resources," 2018 IEEE Electronic Power Grid (eGrid), 2018, pp. 1-6.

[18] L. Callegaro, G. Konstantinou, C. A. Rojas, N. F. Avila and J. E.Fletcher, "Testing Evidence and Analysis of Rooftop PV Inverters Response to Grid Disturbances," *IEEE Journal of Photovoltaics*, vol.10, no. 6, pp. 1882-1891, 2020.

[19] P. Bountouris, I. Abdulhadi, A. Dysko and F. Coffele, "Characterising Grid Connection Stability of Low Voltage PV Inverters through Real- time Hardware Testing," *in CIRED Conference*, Madrid, Spain, 2019.

[20] W. Wang and F. d. Len, "Quantitative Evaluation of DER Smart Inverters for the Mitigation of FIDVR in Distribution Systems," *IEEE Transactions on Power Delivery*, vol. 35, no. 1, 2020.

[21] R. J. Bravo, R. Yinger, S. Robles and J. H. Eto, "FIDVR in distribution circuits," *in IEEE Power & Energy Society General Meeting*, Vancouver,BC, Canada, 21-25 July 2013.

[22] "1,200 MW Fault Induced Solar Photovoltaic Resource Interruption Disturbance Report," *North American Electric Reliability Corporation* (NERC), June 2017.

[23] "900 MW Fault Induced Solar Photovoltaic Resource Interruption Disturbance Report," *Joint NERC and WECC Staff Report*, February 2018.

[24] J. H. Eto, E. Stewart, T. Smith, M. Buckner, H. Kirkham, F. Tuffner and Schoenwald, "Scoping Study on Research and Development Prioritiesfor Distribution-System Phasor Measurement Units," *Lawrence BerkeleyNational Laboratory*, 2015.

[25] A. V. Meier, E. Stewart, A. McEachern, M. Andersen and L.Mehrmanesh, "Precision Micro-Synchrophasors for Distribution Systems: A Summary of Applications," *IEEE Transactions on Smart Grid*, vol. 8, no. 6, 2017.

[26] "IEEE/IEC International Standard - Measuring relays and protection equipment - Part 118-1: Synchrophasor for power systems - Measurements," *IEC/IEEE 60255-118-1:2018* (Revision of C37.118-2005).

[27] "Detailed specifications of the terrestrial radio interfaces of International Mobile Telecommunications-2020 (IMT-2020)", 3GPP, Feb. 2021

[28] A. Osseiran, S. Parkvall, P. Persson, A. Zaidi, S. Magnusson, and K. Balachandran, "5G wireless access: an overview," Ericsson White Paper 1/28423-FGB1010937 April 2020.

[29] M. Cosovic, A. Tsitsimelis, D. Vukobratovic, J. Matamoros and C. Anton-Haro, "5G Mobile Cellular Networks: Enabling Distributed State Estimation for Smart Grids," in *IEEE Communications Magazine*, vol. 55, no. 10, pp. 62-69, Oct. 2017.

[30] M. Gheisarnejad, M. Khooban and T. Dragičević, "The Future 5G Network-Based Secondary Load Frequency Control in Shipboard Microgrids," in IEEE *Journal of Emerging and Selected Topics in Power Electronics*, vol. 8, no. 1, pp. 836-844, March 2020.

[31] M. Hojabri, U. Dersch, A. Papaemmanouil, and P. Bosshart, "A Comprehensive Survey on Phasor Measurement Unit

Applications in Distribution Systems," *Energies* 2019, 12, 4552. https://doi.org/10.3390/en12234552

[32] "IEEE Standard for Synchrophasor Data Transfer for Power Systems," *IEEE Std C37.118.2-2011*.